0026-895X/10/7805-795–803$20.00
MOLECULAR PHARMACOLOGY
Copyright © 2010 The American Society for Pharmacology and Experimental Therapeutics
Mol Pharmacol 78:795–803, 2010

Vol. 78, No. 5
65920/3627993
Printed in U.S.A.

Different N-Terminal Motifs Determine Plasma Membrane Targeting of the Human Concentrative Nucleoside Transporter 3 in Polarized and Nonpolarized Cells[S]

Ekaitz Errasti-Murugarren,[1] F. Javier Casado, and Marçal Pastor-Anglada

Departament de Bioquímica i Biologia Molecular, Facultat de Biologia and IBUB - Institut de Biomedicina de la Universitat de Barcelona, Universitat de Barcelona, Spain; and Centro de Investigación Biomédica en Red-Enfermedades Hepáticas y Digestivas, Barcelona, Spain

Received April 27, 2010; accepted July 19, 2010

ABSTRACT

Human concentrative nucleoside transporter 3 (hCNT3) is a broad-selectivity, high-affinity protein implicated in the uptake of most nucleoside-derived anticancer and antiviral drugs. Regulated trafficking of hCNT3 has been recently postulated as a suitable way to improve nucleoside-based therapies. Moreover, the recent identification of a putative novel hCNT3-type transporter lacking the first 69 amino acids and retained at the endoplasmic reticulum anticipated that the N terminus of hCNT3 contains critical motifs implicated in trafficking. In the current study, we have addressed this issue by using deletions and site-directed mutagenesis and plasma membrane expression and nucleoside uptake kinetic analysis. Data reveal that 1) a segment between amino acids 50 and 62 contains plasma membrane-sorting determinants in nonpolarized cells; 2) in particular, the Val^{57}-Thr^{58}-Val^{59} tripeptide seems to be the core of the export signal, whereas acidic motifs upstream and downstream of it seem to be important for the kinetics of the process; and 3) in polarized epithelia, the β-turn-forming motif ^{17}VGFQ^{20} is necessary for proper apical expression of the protein.

Introduction

Nucleosides play an important role as metabolic precursors in nucleic acid synthesis, being recycled through salvage pathways, and are crucial for the control of cell and tissue growth. In addition, many nucleoside analogs are currently used in anticancer and antiviral therapies, thus highlighting the pharmacological role these molecules can play in disease. Nucleoside-specific membrane transporters mediate plasma membrane permeation of physiologic nucleosides and most nucleoside analogs, which will be further activated intracellularly by nucleoside kinases (Pastor-Anglada et al., 2008; Huber-Ruano and Pastor-Anglada, 2009; Molina-Arcas et al., 2009). Among these transporters, hCNT3 seems to play a crucial role in the disposition of physiological nucleosides and nucleoside analogs because of its broad substrate selectivity, high concentrative capacity, and relatively wide tissue distribution (Ritzel et al., 2001; Errasti-Murugarren et al., 2009). In absorptive epithelia, apical localization of hCNT3 is crucial to determine vectorial flux of all antiviral and anticancer nucleosides tested so far (Errasti-Murugarren et al., 2007), thus being a major candidate to modulate drug pharmacokinetics. It is noteworthy that in chronic lymphocytic leukemia (CLL) cells, hCNT3 protein is expressed but mostly in intracellular compartments; its abundance marks a poorer prognosis in terms of time to disease progression (Mackey et al., 2005). Considering that patients with CLL are treated with fludarabine, an hCNT3 substrate, resistance to treatment could be due in part to impaired trafficking of hCNT3 into the plasma membrane of B cells. In this regard, a recent report from our group showed that retinoic acid increases hCNT3 trafficking to the plasma membrane by transforming growth factor-β1-dependent mechanisms in CLL-derived cell lines, which would eventually contribute to promote fludarabine-induced cytotoxicity (Fernández-Calotti and Pastor-Anglada, 2010). Despite the probable pharmacological relevance of nucleoside transporter trafficking mechanisms, this issue has been poorly addressed so far. In this regard, a previous

This research was supported in part by Centro de Investigación Biomédica en Red (an initiative of Instituto de Salud Carlos III); Generalitat de Catalunya [Grant 2009SGR624]; and the Ministerio de Ciencia e Innovación [Grant BFU2006-07556/BFI], SAF2008–00577].

[1] Current affiliation: Institut de Recerca Biomèdica (IRB), Barcelona, Spain

Article, publication date, and citation information can be found at http://molpharm.aspetjournals.org.
doi:10.1124/mol.110.065920.

[S] The online version of this article (available at http://molpharm.aspetjournals.org) contains supplemental material.

ABBREVIATIONS: CLL, chronic lymphocytic leukemia; hCNT3, human concentrative nucleoside transporter 3; MDCK, Madin-Darby canine kidney cells; ER, endoplasmic reticulum; GFP, green fluorescent protein.

study from our group reported that bile acids can increase plasma membrane concentrative nucleoside transporter 2-related activity by a short-term mechanism consistent with transporter recruitment from intracellular stores into the plasma membrane (Fernández-Veledo et al., 2006).

A novel hCNT3-type transporter (hCNT3ins) has been identified. hCNT3ins lacks the first 69 amino acids of the cytoplasmic N terminus, seems to be the result of alternative splicing of the *SLC28A3* gene, and is retained intracellularly at the endoplasmic reticulum when expressed in nonpolarized cells (Errasti-Murugarren et al., 2009). Expression in polarized MDCK cells also reveals a loss of fidelity for apical sorting (Errasti-Murugarren et al., 2009). These findings anticipate that the N terminus of hCNT3 is implicated in protein trafficking in both polarized and nonpolarized cells. In this regard, several classes of ER export signals in the cytoplasmic domains of proteins have been identified and include, for instance, two adjacent hydrophobic residues or diacidic motifs, although signals can also be conformational epitopes (Nishimura and Balch, 1997; Votsmeier and Gallwitz, 2001; Otte and Barlowe, 2002; Mancias and Goldberg, 2007; Zuzarte et al., 2007).

Unveiling the constitutive and regulated trafficking mechanisms of hCNT-type proteins, thereby controlling cell surface expression of these drug transporters, might help us to better understand how the uptake of natural nucleosides and clinically relevant nucleoside analogs is regulated in the short-term. As a first step in this goal, and on the basis of the evidence obtained when analyzing hCNT3ins localization, in the present study we have constructed a series of truncated and mutated hCNT3 proteins to identify targeting motifs implicated in transporter sorting, both in polarized and nonpolarized cells. In fact, a novel 13-mer comprising two putative diacidic motifs with a region in the middle with alternated hydrophilic and hydrophobic amino acids has been identified as a key determinant of plasma membrane sorting and ER export in nonpolarized cells. It is noteworthy that an additional motif, a tetrapeptide that may adopt a β-turn secondary structure, has also been identified as a molecular determinant for apical sorting of hCNT3 in polarized MDCK cells. These experiments provide novel information about the residues that contribute to the protein localization and ER export, suggesting as well the evidence that key differences exist in sorting mechanisms between polarized and nonpolarized cells.

Materials and Methods

Reagents. Uridine ([5,6-^{3}H]; 35–50 Ci/mmol) was purchased from GE Healthcare (Little Chalfont, Buckinghamshire, UK). Uridine was obtained from Sigma-Aldrich (Saint Louis, MO, USA).

Construction of GFP-Fused Mutants of hCNT3 cDNA. Wild-type human CNT3 cDNA was subcloned into the green fluorescent protein (GFP) vector pEGFPC1/N1 (Clontech, Palo Alto, CA) as described previously (Errasti-Murugarren et al., 2007). The truncated hCNT3-pEGFP constructs were generated using the specific primer combinations defined in Supplemental Tables 1 and 2 under polymerase chain reaction conditions outlined previously (Errasti-Murugarren et al., 2008). Polymerase chain reaction products and the pEGFP vector were double-digested with PstI and HindIII, and the products were gel-isolated and ligated together to generate in-frame fusion proteins with enhanced GFP fused to the N or C terminus of each construct. The QuikChange site-directed mutagenesis kit (Stratagene, La Jolla, CA) was used to generate hCNT3 sorting signal mutants according to the manufacturer's protocol. The GFP-fused hCNT3 chimera was used as template. Specific primer sequences are shown in Supplemental Table 3. All constructions were verified by DNA sequencing and used for transient transfection.

Cell Culture and Transfection. HeLa cells were mantained at 37°C/5% CO_2 in Dulbecco's modified Eagle's medium (Lonza, Basel, Switzerland) supplemented with 10% (v/v) fetal bovine serum, 50 units/ml penicillin, 50 μg/ml streptomycin, and 2 mM L-glutamine. HeLa cells were transiently transfected with plasmid constructions mentioned above with the use of Lipofectamine 2000 (Invitrogen, Carlsbad, CA) following the manufacturer's protocol. Nucleoside transport, confocal microscopy, and flow cytometry analyses were carried out 24, 48, and 72 h after transfection. MDCK cells were also maintained at 37°C/5% CO_2 in Dulbecco's modified Eagle's medium (Lonza) supplemented with 10% fetal bovine serum (v/v), 50 units/ml penicillin, 50 μg/ml streptomycin and 2 mM L-glutamine. Cells were plated in Transwell plates (12-mm diameter, 0.3-μm pore; Costar; Corning Life Sciences, Lowell, MA) and transfected as described previously (Harris et al., 2004).

Nucleoside Transport Assay. Nucleoside uptake was measured as described previously (del Santo et al., 1998) by exposing replicate cultures at room temperature to [^{3}H]labeled uridine (1 μM, 1 μCi/ml; GE Healthcare) in sodium or sodium-free transport buffer (137 mM NaCl or 137 mM choline chloride, 5 mM KCl, 2 mM $CaCl_2$, 1 mM $MgSO_4$, and 10 mM HEPES, pH 7.4). Initial rates of transport were determined using an incubation period of 1 min. Assays were terminated by washing with an excess volume of chilled buffer. Saturation kinetics was evaluated by nonlinear regression analysis and the kinetic parameters derived from this method were confirmed by linear regression analysis of the derived Eadie-Hofstee plots.

Transwell Transport Experiments. The transwell filter inserts were washed three times with sodium or sodium-free buffer, and then 1 μM [^{3}H]uridine (GE Healthcare) was added to the apical or basal side. Transport experiments were conducted with buffer (0.5 ml each in the apical and basal compartments) containing sodium or choline on both sides of the Transwell filters. The transport experiments were terminated by aspirating the buffer, and filters were washed with chilled buffer. The whole filter was wiped with tissue to remove any excess of buffer, and the filter was removed from the plastic support and counted on a scintillation counter. The cells on the filters were solubilized using 0.1% SDS and 100 mM NaOH.

Visualization of Nucleoside Transporters Tagged with Green Fluorescent Protein. To analyze the effect of the mutations on plasma membrane sorting of hCNT3, confocal microscopy of GFP-fused chimeras was performed on a semiconfluent monolayer of transfected HeLa cells cultured on glass coverslips. Glass coverslip-grown cells were rinsed three times with phosphate-buffered saline-Ca^{2+}-Mg^{2+}, fixed for 15 min in 3% paraformaldehyde and 0.06 M sucrose, rinsed three times with phosphate-buffered saline, and then mounted with aqua-poly/mount coverslipping medium (Polysciences, Inc. Warrington, PA). Endoplasmic reticulum retention was analyzed by cotransfecting GFP-fused transporter chimeras with pDsRed2-ER (BD Living Colors). Sections were viewed using a Leica TCS SP5 laser-scanning confocal microscope (Leica Microsystems Heidelberg GmbH, Mannheim, Germany) equipped with a DMI6000 inverted microscope, diode-pumped solid-state (561 nm) argon laser, and a 63× oil immersion objective lens (numerical aperture 1.4) was used. For visualization of GFP and pDsRed2-ER labelings, images were acquired sequentially using 488 and 561 nm laser lines, Acousto-Optical Beam Splitter, emission detection ranges from 500 to 550 and 571 to 650 nm, respectively, and the confocal pinhole set at 1 Airy unit. Optical sections were collected every 0.3 μm in a 1024 × 1024 format, zoom 4 and pixel size 60 × 60 nm. Transfection efficiency as well as fluorescence intensity were determined by

flow cytometry using a Cytomics FC 500 MPL Flow Cytometry System (Beckman Coulter, Fullerton, CA).

To analyze the polarized membrane sorting of GFP-fused hCNT3 and hCNT3 mutants, 1.7×10^5 MDCK cells were grown in 12-well Corning Costar polycarbonate transwell filter inserts for 24 h and then transfected as explained previously. The filters were rinsed three times with phosphate-buffered-Ca^{2+}-Mg^{2+}, fixed for 15 min in 3% paraformaldehyde and 0.06 M sucrose, excised, and then loaded on a glass slide and covered with a coverslip. Between the slide and the coverslip, a ~1-mm gap was filled with aqua-poly/mount coverslipping medium (Polysciences, Inc. Warrington, PA). Actin was stained using phalloidin-TRITC (Sigma-Aldrich, Saint Louis, MO, USA). Images were also obtained using a Leica TCS SP5 laser scanning confocal microscope (Leica Microsystems Heidelberg GmbH, Manheim, Germany). Optical sections were collected every 0.3 μm in a 1024×1024 format, zoom 4 and pixel size 60×60 nm.

Data Analysis. Data are expressed as the mean ± S.D. of uptake values obtained in three wells or filter inserts. Data are representative of three experiments carried out on different days on different batches of cells.

Results

Deletion of the Cytoplasmic N Terminus of hCNT3 Causes ER Retention in a Nonpolarized Cell Model. To gain insight into the signal sequence(s) required for targeting of hCNT3 to the plasma membrane in a nonpolarized cell model, we employed a truncation approach, in which the full-length protein was progressively shortened from the N terminus. hCNT3 mutants fused to the N or C terminus of the GFP were generated and transiently expressed in the HeLa cell line, and the subcellular distribution and kinetic properties of each truncation mutant were determined 24 h after transient transfection. HeLa cells were transfected with the plasmids coding for the wild-type GFP-hCNT3, GFP-hCNT3Δ35, GFP-hCNT3Δ49, GFP-hCNT3Δ58, GFP-hCNT3Δ62, or GFP (Fig. 1). Functional characterization of these constructions resulted in a significant sodium-dependent uridine transport activity for the wild-type, and the 35 and 49 amino acid-deleted mutants, whereas GFP-hCNT3Δ62 expressing HeLa cells showed no sodium-dependent uridine transport activity. On the other hand, the GFP-hCNT3Δ58 construction showed a slightly higher uridine sodium-dependent activity than that shown by HeLa cells transfected with the GFP vector (Fig. 1B). Confocal microscopy analysis of transfected HeLa cells showed that truncation of 35 and 49 amino acids had no effect on plasma membrane sorting, whereas truncation of 62 amino acids resulted in ER retention of the transporter. The deletion of 58 amino acids resulted in both ER retention and little but significant plasma membrane localization (Fig. 1C). The intracellular localization of these chimeras was determined by cotransfection of GFP-fused hCNT3 truncation mutants with pDsRed2-ER, a specific

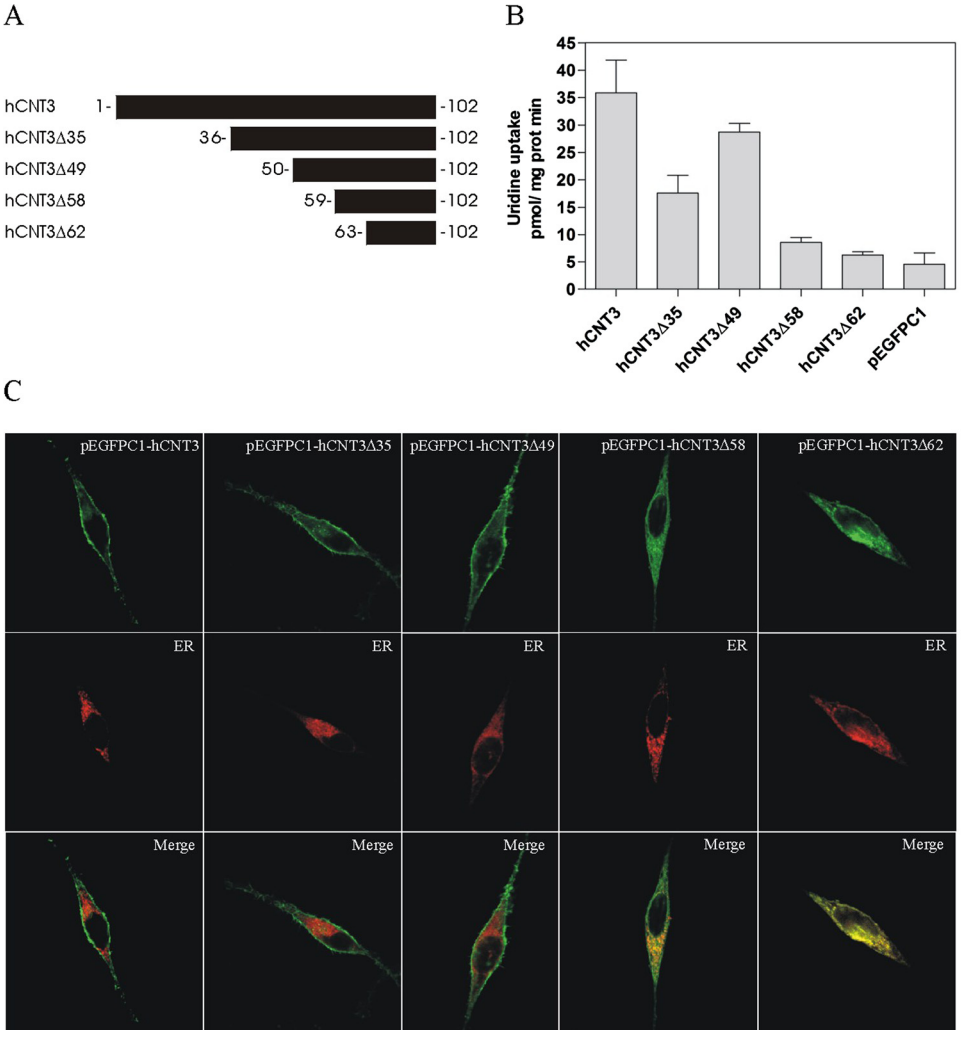

Fig. 1. Summary of the mutations made in the N terminus of hCNT3 and their effects on plasma membrane expression and activity in HeLa cells. A, schematic representation of the N terminus of hCNT3 (residues 1–102) and truncation mutants. B, sodium-dependent uptake of [^{3}H]uridine (1 μM, 1 min) by GFP-hCNT3 and GFP-fused truncation mutants was measured in transport medium containing 137 mM NaCl or 137 mM choline chloride. Sodium-dependent transport was calculated as uptake in NaCl medium minus uptake in choline chloride. Data are expressed as the mean ± S.D. of three experiments carried out on different days on different batches of cells. C, subcellular localization of GFP-fused hCNT3 truncation mutants in HeLa cells compared with that of the full-length GFP-hCNT3 protein (691 amino acids). Wild-type hCNT3 and truncation mutants hCNT3Δ35 and hCNT3Δ49 are expressed at the plasma membrane, showing no overlap with pDsRed2-ER expression, a protein expressed in the endoplasmic reticulum. On the other hand, truncation mutant hCNT3Δ62 colocalizes with pDsRed2-ER staining, indicating that this mutant is retained in the endoplasmic reticulum. Deletion of first 58 amino acids from N terminus of hCNT3 (hCNT3Δ58) resulted in an intermediate pattern, both ER and plasma membrane being stained.

marker of the ER. As shown in Fig. 1C, wild-type hCNT3 and 35- and 49-amino acid truncated mutants did not colocalize with the ER marker, being mainly expressed at the cell surface, whereas the 62-amino acid truncated mutant and most but not all of the 58-amino acid deleted mutant showed a distribution pattern coincident with the ER marker. Moreover, flow cytometry analysis revealed similar transfection rates for all constructions but slight differences in fluorescence intensity values (Table 1). Kinetic analysis of the plasma membrane expressed mutants showed no differences in uridine affinity (Supplemental Fig. 1), which suggests that the N terminus of the transporter is not involved in substrate specificity. The calculation of V_{max}/fluorescence intensity ratios for each construction corroborated proper membrane sorting for both the 35 and 49 amino acids truncated constructions and intracellular retention of the 58 amino acid truncation (Table 1). In all cases results were identical with those of the N1GFP- or C1GFP-fused chimeras (data not shown).

A 13-Residue Peptide of the hCNT3 N Terminus Is Involved in the ER Export and Plasma Membrane Sorting in a Nonpolarized Cell Model. These results demonstrate that amino acids between 50 and 62 are important for cell surface targeting. This 13-residue peptide comprised two acidic motifs (residues ^{53}DEE^{55} and ^{60}EQD^{62} of the human CNT3 sequence) with a region in the middle with alternated hydrophilic and hydrophobic amino acids (residues ^{56}QVTV^{59}). These motifs are conserved in the N terminus of the concentrative nucleoside transporter 3 from several species (Fig. 2A). To identify further the potential role of these domains in the export of CNT3 protein from the ER, we generated a series of mutants in which each amino acid of the sequence ^{50}TKQDEEQVTVEQD^{62} was substituted by an alanine individually or in combination (Fig. 2B). Wild-type and hCNT3 mutants conjugated with GFP were transiently expressed in HeLa cells, and their activities and subcellular localization were revealed by uptake assays and confocal microscopy, respectively (Fig. 2, B and C). Individual mutation of residue Tyr^{50}, Lys^{51}, Gln^{52}, Asp^{53}, Glu^{54}, Glu^{55}, Gln^{56}, Gln^{61}, or Asp^{62} did not significantly influence the activity and subcellular localization of hCNT3 mutants after a 24-h culture (Fig. 2, B and C). In contrast, single mutations of Val^{57}, Thr^{58}, Val^{59}, and Glu^{60} abolished transporter activity and were associated with intracellular ER retention (Fig. 2, B–D). Nevertheless, the sodium-dependent uridine transport measured 48 h after transfection reached values similar to those observed for the wild-type construction (Supplemental Fig. 2A). In this regard, analysis of the activity and subcellular localization 48 h after transfection revealed a clearly distinguishable plasma membrane localization of the mutants (Supplemental Fig. 2B), suggesting that these mutations did not completely block but rather slowed down the delivery of hCNT3 to the plasma membrane. Substitution of Val^{57} and/or Val^{59} with isoleucine had no effect on transporter activity and subcellular localization (data not shown). Because the presence of acidic motifs has been suggested to be essential for cell-surface expression of several plasma membrane proteins (Nishimura and Balch, 1997; Votsmeier and Gallwitz, 2001; Zuzarte et al., 2007), we determined the effect of either double or triple mutations of Asp^{53}-Glu^{55} on hCNT3 activity and subcellular localization. Our results indicate that, although individual mutation of Asp^{53}, Glu^{54}, or Glu^{55} had no obvious effect on transporter export from ER, double and triple mutations of acidic residues to alanine resulted in intracellular ER retention and dramatic loss of plasma membrane sodium-dependent uridine transport activity (Fig. 2, B and C). In this case, these changes also seemed to be the result of slow trafficking, because proper sodium-dependent uridine uptake and plasma membrane localization were revealed 48 h after transfection (Supplemental Fig. 2, A and B). However, mutation of tripeptide Val^{57}-Thr^{58}-Val^{59} to Ala^{57}-Ala^{58}-Ala^{59} resulted in a complete retention of the transporter in the ER even at 72 h after transfection (Supplemental Fig. 2, A and B). This observation suggests that these amino acids are the core of the hCNT3 ER export signal and that the acidic motifs upstream and downstream of this core region are important for the kinetics of the sorting process. Results were identical in all cases with either the N1GFP- or the C1GFP-fused chimeras (data not shown).

The Cytoplasmic N Terminus of hCNT3 Contains an Apical Targeting Signal. As introduced above, concentrative nucleoside transporter-type proteins show an asymmetrical distribution in polarized cells, being present at the apical surface and determining vectorial flux of nucleosides (Ngo et al., 2001; Errasti-Murugarren et al., 2007). Because deletion of the first 69 amino acids from the N terminus of hCNT3 results in mis-sorting of the transporter protein in polarized cells (Errasti-Murugarren et al., 2009), a series of truncation mutants was also generated to define the specific requirements for normal apical localization of hCNT3. Polarized MDCK cells were transfected with the plasmids coding for GFP-fused hCNT3, hCNT3Δ10, hCNT3Δ25, hCNT3Δ69, or GFP. The steady-state membrane distribution of these mutants was determined by activity assays on polarized MDCK cells grown on Transwell inserts (Fig. 3B) and confirmed using immunofluorescence confocal microscopy of fixed monolayers (Fig. 3C). These data confirmed that hCNT3 was present in the apical domain of polarized MDCK. Deletion of the first 10 amino acids from the N terminus of hCNT3 had no effect on transporter apical sorting, whereas deletion of

TABLE 1

Transfection efficiency and fluorescence intensity of GFP-fused chimeras

HeLa cells were transfected with the GFP-fused chimeras; after 24 h, cells were resuspended and analyzed by flow cytometry for transfection efficiency and construction expression rate. The calculated V_{max} values (obtained from Supplemental Figure 2) were normalized to the fluorescence intensity values. Fluorescence intensity is expressed in arbitrary units. Data are expressed as the mean ± S.D. of three experiments carried out on different days on different batches of cells.

Construction	Transfection	S.D.	Fluorescence Intensity	S.D.	Ratio V_{max}/Fluorescence Intensity
	%				
hCNT3	77.9	5.1	223.4	17	2.1
hCNT3Δ35	81.9	3.9	129.5	9.5	1.9
hCNT3Δ49	82.2	2.2	196.7	4.1	2.1
hCNT3Δ58	79.9	3.7	188.4	7.3	0.3

either 25 or 69 amino acids resulted in a similar missorting of hCNT3. In fact, both deleted constructs resulted in a significant reduction of the apical and a concomitant increase of the basolateral sodium-dependent uridine transport (Fig. 3B). Moreover, flow cytometry analysis showed the same transfection rates but different fluorescence intensity values for all constructions (Table 2), being the hCNT3 truncated mutant activities corrected by their fluorescence intensities (Table 3). All together, these data identified a sequence of 15 amino acids (^{11}AEGYSNVGFQNEENF^{25}) that seems to be important for polarized expression of hCNT3 in MDCK cells. In all cases, results

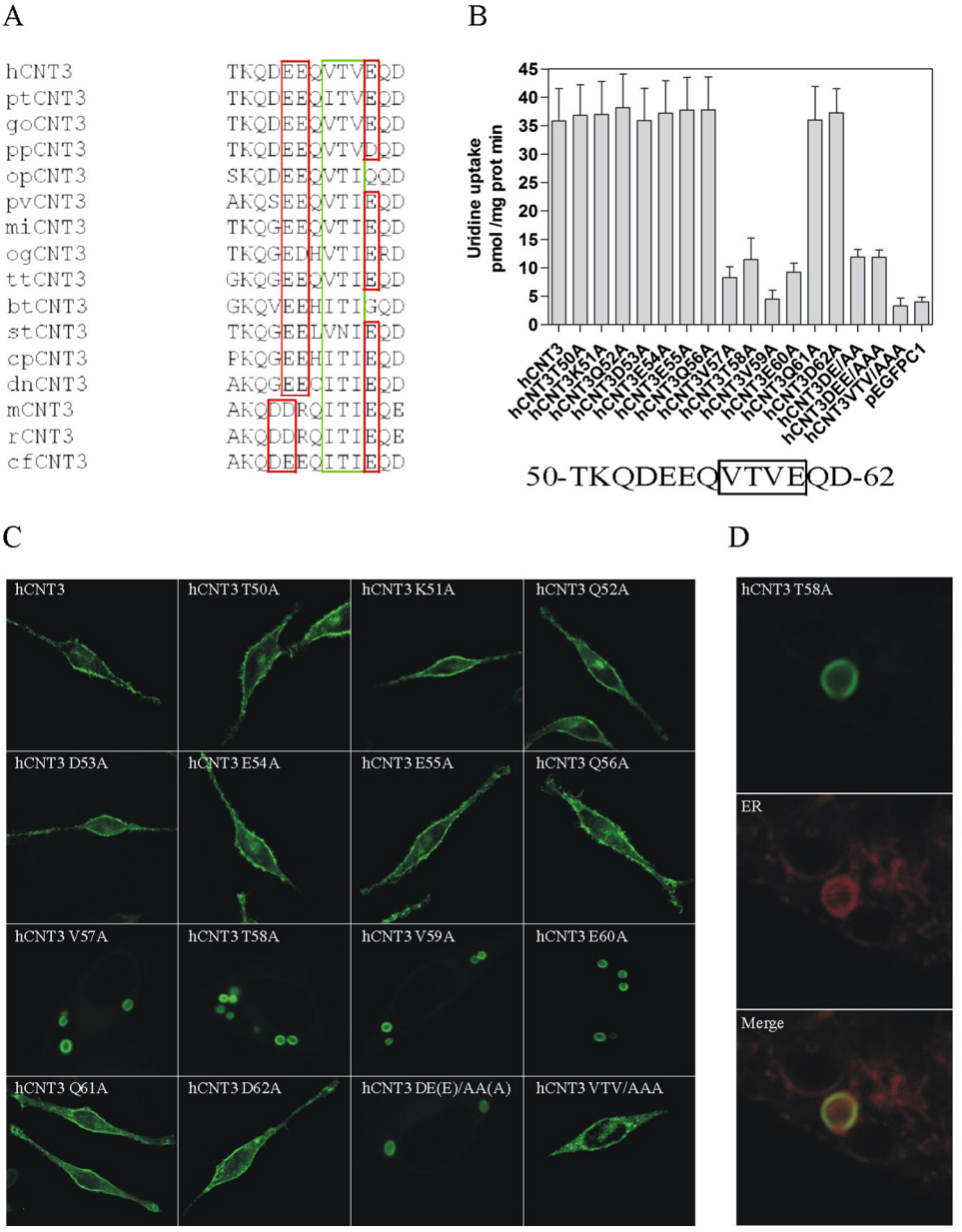

Fig. 2. An N-terminal motif dictates plasma membrane sorting in HeLa cells. A, primary structure of human CNT3 (residues 50–62). The amino acid sequence of human CNT3 (hCNT3, GenBank accession number AF305210) is compared with that of chimpanzee (ptCNT3, Ensembl accession number ENSDNOP00000046380), gorilla (goCNT3, Ensembl accession number ENSDNOP00000001197), orangutan (ppCNT3, Ensembl accession number ENSDNOP00000021660), pika (opCNT3, Ensembl accession number ENSDNOP00000003345), megabat (pvCNT3, Ensembl accession number ENSDNOP00000006777), mouse lemur (miCNT3, Ensembl accession number ENSDNOP00000009061), bush baby (ogCNT3, Ensembl accession number ENSDNOP00000002294), dolphin (ttCNT3, Ensembl accession number ENSDNOP00000004747), cow (btCNT3, Ensembl accession number ENSBTAP00000024328), squirrel (stCNT3, Ensembl accession number ENSSTOP00000014307), guinea pig (cpCNT3, Ensembl accession number ENSCPOP00000011872), armadillo (dnCNT3, Ensembl accession number ENSDNOP00000003788), mouse (mCNT3, GenBank accession number AF305211), rat (rCNT3, GenBank accession number AY059414), and dog (cfCNT3, Ensembl accession number ENSDNOP00000001980). Suggested important domains are boxed. B, sodium-dependent uptake of [^{3}H]uridine (1 μM, 1 min) by GFP-hCNT3 and GFP-fused alanine substitution mutants was measured as in Fig. 1. Suggested important domain is boxed. Data are expressed as the mean ± S.D. of three experiments carried out on different days on different batches of cells. C, subcellular localization of wild-type GFP-hCNT3 and GFP-fused alanine substitution mutants in HeLa cells. Wild-type hCNT3 and mutants hCNT3T50A, K51A, Q52A, D53A, E54A, E55A, Q56A, Q61A, and D62A are expressed at the plasma membrane, showing no overlap with ER marker pDsRed2-ER. On the other hand, hCNT3V57A, T58A, V59A, ^{53}DE^{54}/AA, and ^{53}DEE^{55}/AAA mutants were retained in intracellular ER derived structures. Finally, hCNT3^{57}VTV^{59}/AAA mutant colocalizes with pDsRed2-ER staining, indicating that this mutant is retained in the endoplasmic reticulum. D, detailed intracellular ER derived structure from mutant hCNT3T58A and its colocalization with ER marker pDsRed2-ER.

were identical with either the N1GFP- or the C1GFP-fused chimeras (data not shown).

A Tetrapeptide Adopting a β-Turn Structure Is Implicated in Apical Sorting of hCNT3. The analysis of the 15-residue long peptide sequence showed no evident structural motifs, apart from a clustering of negatively charged amino acids in the distal part of the sequence. The alignment of this amino acid sequence with the equivalent one from different CNT3 orthologs showed a low conservation degree among different species (Fig. 4A). Several short cytosolic motifs have been identified as positive apical sorting or ER export signals in polarized models. Among these, Sun et al. (2003) defined a fourteen amino acid sequence required for optimal apical membrane targeting of the rat ileal bile acid transporter, with a β-turn tetramer within this sequence sufficient to produce an apical bias of protein location. On the basis of this report, we analyzed the conformational topology of these selected 15 amino acids of the hCNT3 N terminus applying a predictive method to identify β-turns within proteins named tetrapeptide residue-coupled model, developed by Chou (1997). Using this method successive tetrapeptide regions along the N-terminal region of hCNT3 were analyzed for propensity to form β-turns, scored in terms of a discriminant function δ, where values greater than 0 indicate the tetrapeptide forms a β-turn. Within the 15-amino acids long peptide identified using the truncation approach of the cytoplasmic N terminus of hCNT3, we found one tetrapeptide that scored positively for the occurrence of a β-turn (^{17}VGFQ^{20}) (Fig. 4C). Similar β-turn-forming tetrapeptides were found within the corresponding 15-residue long peptide of some but not all of the orthologs analyzed, suggesting a common mechanisms of apical sorting for some CNT3 orthologs (Fig. 4C). In addition, substitution of the putative cytosolic β-turn domain with a similar but non–β-turn-forming tetrapeptide Met-Thr-Phe-Arg (MTFR) (Chou, 1997) resulted in a similar phenotype to that previously observed for the deletion of 25 and 69 amino acids, with a reduction in the apical and an increase in the basolateral sodium-dependent uridine transport activity (Fig. 4B). The steady-state membrane distribution of these mutants was confirmed using immunofluorescence confocal microscopy of fixed monolayers (Fig. 4D). Moreover, flow cytometry analysis showed similar transfection rates and fluorescence intensity values for all constructions. hCNT3 mutant activities were corrected by their fluorescence intensities to allow better comparisons (Table 3). In all cases, results were identical with the N1GFP- or C1GFP-fused chimeras (data not shown).

Discussion

In the present contribution, N-terminally truncated mutants of hCNT3 have been used to reveal that 1) the N terminus was not implicated in substrate binding, which is in agreement with previous data (Loewen et al., 1999; Hamilton

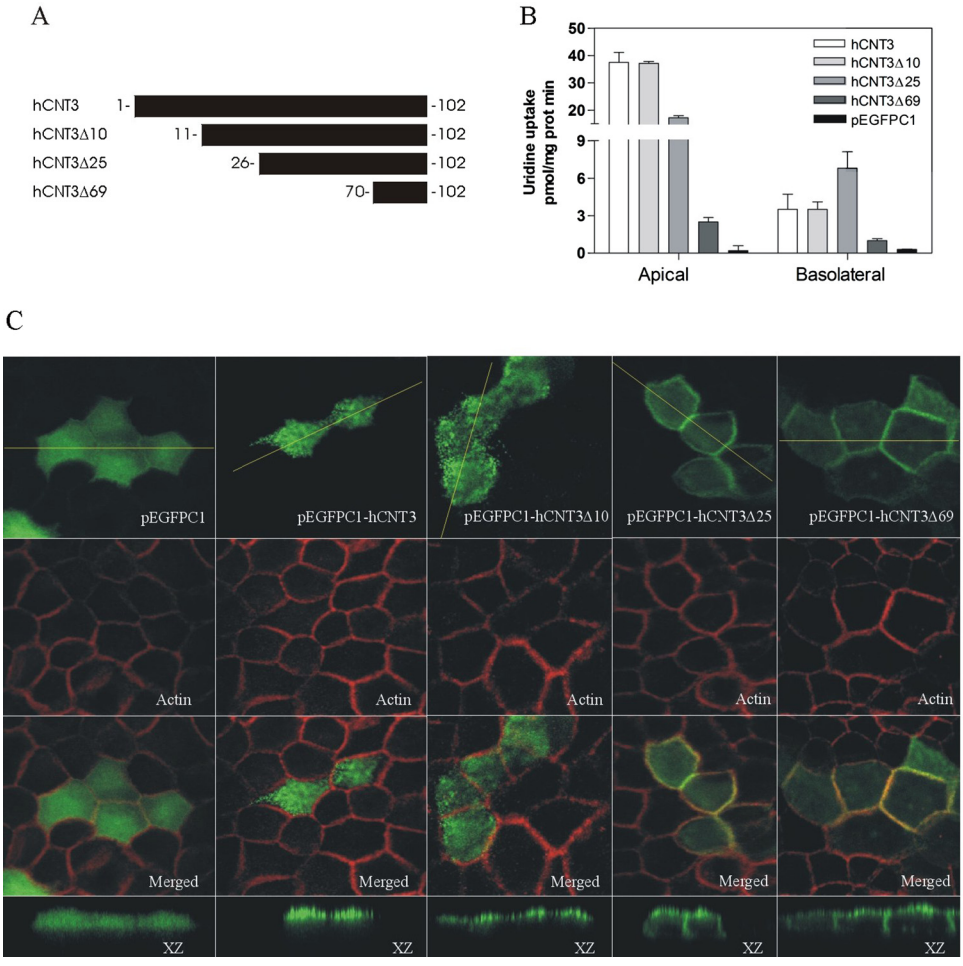

Fig. 3. Summary of the mutations made in the N terminus of hCNT3 and their effects on plasma membrane expression and activity in MDCK cells. A, schematic representation of the N terminus of hCNT3 (residues 1–102) and truncation mutants. B, apical and basal sodium-dependent uptake of [^{3}H]uridine (1 μM, 1 min) by GFP-hCNT3 and GFP-fused truncation mutants was measured in transport medium containing 137 mM NaCl or 137 mM choline chloride. Sodium-dependent transport was calculated as uptake in NaCl medium minus uptake in choline chloride. Data are expressed as the mean ± S.D. of three experiments carried out on different days on different batches of cells. C, transiently transfected MDCK cells with GFP-tagged hCNT3, hCNT3 truncation mutants, or vector alone. Cells were fixed, stained for actin with Texas Red conjugated phalloidin, and visualized by confocal microscopy. Red, actin; green, GFP. Subcellular localization of hCNT3 truncation mutants in MDCK cells was compared with that of the full-length hCNT3 protein (691 amino acids). Wild-type hCNT3 and truncation mutant hCNT3Δ10 are sorted to the apical plasma membrane, showing no basolateral staining. On the other hand, truncation mutants hCNT3Δ25 and Δ69 showed both apical and basolateral staining.

et al., 2001) and 2) a 13-residue peptide between amino acids 50 and 62 contained plasma membrane sorting determinants in nonpolarized cell models. Alanine scanning mutagenesis of this region revealed the presence of two different domains essential for proper plasma membrane sorting of the transporter, a PDZ binding domain type II-like sequence and negatively charged amino acids upstream and downstream of this core region. This particular amino acid distribution is highly conserved in all CNT3 orthologs, suggesting a common mechanism for CNT3 protein sorting in nonpolarized cell models. Individual mutations of ^{57}VTV^{59} to alanines resulted in intracellular ER-derived structures retention of hCNT3 transporter mutants 24 h after transfection. One possible explanation of these structures is that vesicles budding from ER and containing hCNT3 mutants leave ER and fuse homotypically to give rise to larger containers, as described for GABA transporter-1 mutants (Farhan et al., 2008). However, in contrast to those described for GABA transporter-1 mutants, these ER-derived structures are not a dead-end for hCNT3 mutants because they are able to reach the plasma membrane 48 h after transfection. In addition, mutation of ^{57}VTV^{59} to ^{57}AAA^{59} resulted in ER retention of the mutant, suggesting an essential role for this domain in the ER export of the hCNT3 transporter.

Replacement of either Val^{57} or Val^{59} with other nonpolar amino acids, similar to those found in other orthologs, resulted in a fully active hCNT3 transporter, showing that it was the hydrophobic nature of valine that leads to efficient ER export. The importance of hydrophobic residue-based sorting signals has been described in the interaction of transmembrane cargo with COPII components (Otte and Barlowe, 2002) as well as in protein-protein interactions occurring at the plasma membrane. In this regard, three different PDZ domain recognition motifs (classes I–III) depending on valine residues play a role in protein transport to the plasma membrane (Nourry et al., 2003). In addition to the valine, these motifs require a critical amino acid (X) at position −2; in class II, a hydrophobic residue (Ψ) at position −2 (XΨXΨ) in the peptide interacts with a corresponding hydrophobic residue in the PDZ-containing protein (Nourry et al., 2003). In the case of hCNT3, the valine residue in position −2 is also essential for ER export, it being likely that this internal ^{56}QVTV^{59} motif of the transporter is recognized during ER export by PDZ domain containing proteins. Moreover, the role of this sequence in COPII dependent ER export could not be excluded, a possibility that warrants further studies.

Furthermore, our experiments ruled out the importance of diacidic motifs in hCNT3 ER export. In fact, residues ^{53}DEE^{55} and ^{60}EQD^{62} might confer the consensus of the ER export diacidic motif (DE/X/ED). This motif is present in the cytoplasmic tail of several transmembrane proteins (Nishimura et al., 1999; Votsmeier and Gallwitz, 2001; Zuzarte et al., 2007). Individual mutations of negatively charged amino acids from both putative diacidic motifs resulted in fully functional transporters, except for the mutation E60A, which showed an ER-derived structures intracellular retention, as showed for previous hCNT3 mutants. The progressive substitution of negatively charged amino acids by alanines produced a decrease in surface expression and in transport activity of the CNT3 transporter, suggesting the need of at least two negatively charged amino acids preceding the ^{56}QVTV^{59} domain, as well as the Glu^{60} downstream of this domain for transporter export from the ER. This result is in accordance with previous reports showing that the immediate environment of certain motifs affect their function (Mancias and Goldberg, 2007), thus suggesting a role for the acidic residues referred to above in the maintenance of the proper spatial conformation of the ^{56}QVTV^{59} domain. Nevertheless, an additional role for these acidic residues besides the structural one cannot be ruled out.

hCNT3 is also expressed in a variety of epithelia in which its apical sorting and expression might determine vectorial flux of nucleosides and nucleoside-derived drugs (Mangravite et al., 2003; Damaraju et al., 2007; Errasti-Murugarren et al., 2007). In fact, in contrast to basolateral sorting motifs, the interaction of apical sorting determinants of proteins with the sorting machinery of polarized cells is still poorly understood. The known motifs identified so far are highly diverse, often consisting of post-translational modifications or transmembrane domains that enable preferential asso-

TABLE 2

Transfection efficiency and fluorescence intensity of GFP-fused chimeras

MDCK cells were transfected with the GFP-fused chimeras; after 48 h, cells were resuspended and analyzed by flow cytometry for transfection efficiency and construction expression rate. Fluorescence intensity is expressed in arbitrary units. Data are expressed as the mean ± S.D. of three experiments carried out on different days on different batches of cells.

Construction	Transfection	S.D.	Fluorescence Intensity	S.D.
	%			
hCNT3	39.6	0.5	60.3	4.1
hCNT3Δ10	36.4	0.3	61.1	2.9
hCNT3Δ25	36.8	0.5	64.0	0.3
hCNT3Δ69	38.5	0.3	11.0	4.4
hCNT3^{17}VGFQ^{20}MTFR	38.2	0.3	62.2	4.1

TABLE 3

Analysis of the polarized sorting of GFP-fused chimeras

MDCK cells were transfected with the GFP-fused chimeras, and uridine uptake at both apical and basolateral domains was analyzed. GFP-fused transporters sodium-dependent uridine uptake was normalized by fluorescence intensity values from Table 2, and then the ratio between apical and basolateral uridine uptake was calculated. Data are expressed as the mean ± S.D. of three experiments carried out on different days on different batches of cells.

Construction	Apical Activity	Basolateral Activity	Ratios		
			Apical Activity/Fluorescence Intensity	Basolateral Activity/Fluorescence Intensity	Apical/Basolateral
	$pmol \cdot mg\ of\ protein^{-1} \cdot min^{-1}$				
hCNT3	37.5 ± 3.6	3.5 ± 1.2	0.62	0.06	10.3
hCNT3Δ10	37.1 ± 0.7	3.6 ± 0.5	0.60	0.06	10.0
hCNT3Δ25	17.2 ± 0.7	6.9 ± 1.9	0.27	0.11	2.45
hCNT3Δ69	2.9 ± 0.3	1.0 ± 0.2	0.26	0,10	2.60
hCNT3^{17}VGFQ^{20}MTFR	16.8 ± 0.8	7.2 ± 0.8	0.27	0.12	2.25

ciation of the protein with plasma membrane microdomains, being not as strict as prototypical basolateral determinants (Ellis et al., 2006). Moreover, several short cytosolic motifs have been identified as positive apical sorting or ER export signals in polarized models (Karim-Jimenez et al., 2000; Francesconi and Duvoisin, 2002; Sun et al., 2003; Kwon and Guggino, 2004). In fact, nonconserved amino acid sequences in different protein orthologs might define by themselves structural signals for ER export and polarized sorting (Sun et al., 2003; Subramanian et al., 2004; Sun et al., 2004). In this study, we showed that the efficient arrival of hCNT3 to the apical domain of the polarized MDCK cell model requires four amino acids (^{17}VGFQ^{20}) in the proximal segment of the cytosolic amino terminus. The prediction of the secondary structure of the proximal segment of the N terminus of hCNT3 indicated that a potential turn structure may occur between amino acids 17 and 20. In this regard, β-turn-forming peptides have been proposed to be implicated in either basolateral or apical sorting (Aroeti et al., 1993; Sun et al., 2003, 2004; Subramanian et al., 2004). Disruption of this probable β-turn structure by either deletion or site-directed mutagenesis to form a non–β-turn tetrapeptide resulted in partial mis-sorting of hCNT3 from the apical to the basolateral domain, either during secretion or after endocytosis, as described for the cystic fibrosis transmembrane conductance regulator (Moyer et al., 1999). Although the probability of β-turn structure is apparently not conserved in a few orthologs, when their primary sequences were analyzed based upon the tetrapeptide residue-coupled model (Chou, 1997), this does not fully rule out its occurrence. In fact, our data show that this apical sorting signal is necessary but not sufficient to confer polarized apical localization of hCNT3 in MDCK cells. In this regard, some membrane proteins contain multiple sorting signal motifs that are regulated by several sorting factors and mechanisms (Saunders and Limbird, 1997; Pei et al., 2000) suggesting the requirement of complementary signals for proper apical sorting of the hCNT3 transporter.

Understanding mechanisms responsible for hCNT3 traf-

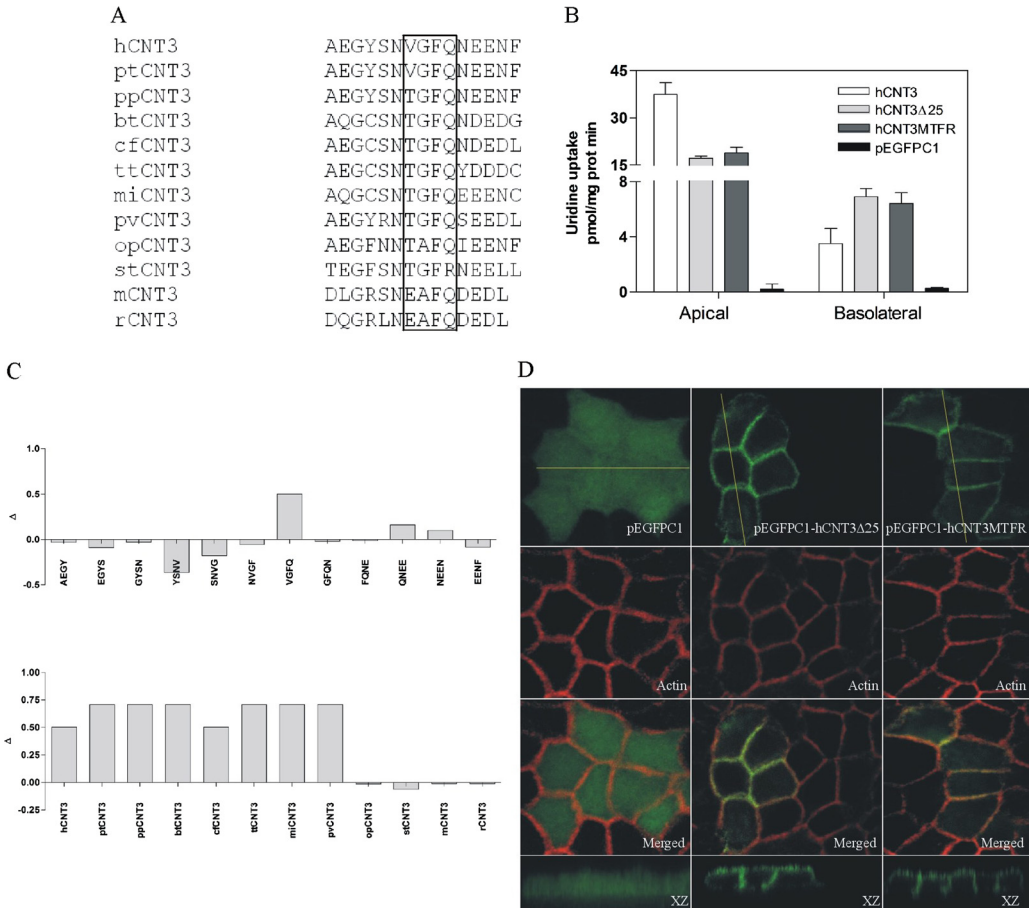

Fig. 4. An N-terminal motif dictates apical sorting of hCNT3. A, primary structure of human CNT3 (residues 11–25). The amino acid sequence of human CNT3 (hCNT3) is compared with that of chimpanzee (ptCNT3), orangutan (ppCNT3), cow (btCNT3), dog (cfCNT3), dolphin (ttCNT3), mouse lemur (miCNT3), megabat (pvCNT3), pika (opCNT3), squirrel (stCNT3), mouse (mCNT3), and rat (rCNT3). Protein accession numbers are the same as in Fig. 2. Suggested β-turn forming tetrapeptide is boxed. B, apical and basal sodium-dependent uptake of [^{3}H]uridine (1 μM, 1 min) by hCNT3 and mutants was measured as in Fig. 3. Data are expressed as the mean ± S.D. of three experiments carried out on different days on different batches of cells. C, application of tetrapeptide residue-coupled model (Chou, 1997) to predict the localization of β-turns within the putative N-terminal targeting region of hCNT3. Sequential tetrapeptides were assigned a β-turn attribute function (Δ), where the criterion for β-turn prediction is $\Delta > 0$. Prediction of occurrence of β-turns in N terminus of hCNT3 (residues 11–25) (top) and hCNT3 orthologs (bottom). D, transiently transfected MDCK cells with GFP-tagged hCNT3 and hCNT3 mutants. Cells were fixed, stained for actin with Texas Red conjugated phalloidin, and visualized by confocal microscopy. Red, actin; green, GFP. Subcellular localization of hCNT3 mutants in MDCK cells was compared with that of the full-length hCNT3 protein (691 amino acids). Wild-type hCNT3 is sorted to the apical plasma membrane, showing no basolateral staining, whereas the non–β-turn-forming hCNT3^{17}VGFQ^{20}MTFR mutant showed both apical and basolateral staining.

ficking may be of biological and pharmacological relevance. hCNT3 is found mostly in intracellular stores in CLL cells and this occurrence is associated with poor prognosis in patients under fludarabine treatment (Mackey et al., 2005; Tsang et al., 2008). We recently found that hCNT3 trafficking into the plasma membrane can be stimulated by retinoic acid in CLL but also in solid tumor-derived cell lines. This phenomenon is mediated by transforming growth factor-β1 and is dependent upon the small GTPase RhoA (Fernández-Calotti and Pastor-Anglada, 2010). It is noteworthy that Rho family members are found in vesicular compartments, where they can play major roles in vesicle trafficking in both endocytic and exocytic pathways (Ridley, 2001; Symons and Rusk, 2003).

In summary, mapping of the N terminus tail of the hCNT3 protein revealed that acidic and hydrophobic motifs in this domain control ER export and cell surface expression levels in nonpolarized cells, whereas a putative β-turn domain contributes to hCNT3 polarized surface expression in epithelial cells. This represents a first step in the understanding of the mechanisms of constitutive and regulated hCNT3 trafficking, which is a relevant goal not only for a better understanding of hCNT3 biology but also in the clinical treatment with nucleoside-derived drugs.

Acknowledgments

We are grateful to the Confocal Microscopy Facility of Serveis Cientificotècnics (Universitat de Barcelona-IDIBAPS) for their support and advice with confocal techniques. We also thank I. Iglesias for technical assistance.

References

Aroeti B, Kosen PA, Kuntz ID, Cohen FE, and Mostov KE (1993) Mutational and secondary structural analysis of the basolateral sorting signal of the polymeric immunoglobulin receptor. *J Cell Biol* **123:**1149–1160.

Chou KC (1997) Prediction of beta-turns. *J Pept Res* **49:**120–144.

Damaraju VL, Elwi AN, Hunter C, Carpenter P, Santos C, Barron GM, Sun X, Baldwin SA, Young JD, Mackey JR, et al. (2007) Localization of broadly selective equilibrative and concentrative nucleoside transporters, hENT1 and hCNT3, in human kidney. *Am J Physiol Renal Physiol* **293:**F200–F211.

del Santo B, Valdés R, Mata J, Felipe A, Casado FJ, and Pastor-Anglada M (1998) Differential expression and regulation of nucleoside transport systems in rat liver parenchymal and hepatoma cells. *Hepatology* **28:**1504–1511.

Ellis MA, Potter BA, Cresawn KO, and Weisz OA (2006) Polarized biosynthetic traffic in renal epithelial cells: sorting, sorting, everywhere. *Am J Physiol Renal Physiol* **291:**F707–F713.

Errasti-Murugarren E, Cano-Soldado P, Pastor-Anglada M, and Casado FJ (2008) Functional characterization of a nucleoside-derived drug transporter variant (hCNT3C602R) showing altered sodium-binding capacity. *Mol Pharmacol* **73:**379–386.

Errasti-Murugarren E, Molina-Arcas M, Casado FJ, and Pastor-Anglada M (2009) A splice variant of the SLC28A3 gene encodes a novel human concentrative nucleoside transporter-3 (hCNT3) protein localized in the endoplasmic reticulum. *FASEB J* **23:**172–182.

Errasti-Murugarren E, Pastor-Anglada M, and Casado FJ (2007) Role of CNT3 in the transepithelial flux of nucleosides and nucleoside-derived drugs. *J Physiol* **582:**1249–1260.

Farhan H, Reiterer V, Kriz A, Hauri HP, Pavelka M, Sitte HH, and Freissmuth M (2008) Signal-dependent export of GABA transporter 1 from the ER-Golgi intermediate compartment is specified by a C-terminal motif. *J Cell Sci* **121:**753–761.

Fernández-Calotti P and Pastor-Anglada M (2010) All-trans-retinoic acid promotes trafficking of human concentrative nucleoside transporter-3 (hCNT3) to the plasma membrane by a TGF-beta1-mediated mechanism. *J Biol Chem* **285:**13589–13598.

Fernández-Veledo S, Huber-Ruano I, Aymerich I, Duflot S, Casado FJ, and Pastor-Anglada M (2006) Bile acids alter the subcellular localization of CNT2 (concentrative nucleoside cotransporter) and increase CNT2-related transport activity in liver parenchymal cells. *Biochem J* **395:**337–344.

Francesconi A and Duvoisin RM (2002) Alternative splicing unmasks dendritic and axonal targeting signals in metabotropic glutamate receptor 1. *J Neurosci* **22:**2196–2205.

Hamilton SR, Yao SY, Ingram JC, Hadden DA, Ritzel MW, Gallagher MP, Henderson PJ, Cass CE, Young JD, and Baldwin SA (2001) Subcellular distribution and membrane topology of the mammalian concentrative Na+-nucleoside cotransporter rCNT1. *J Biol Chem* **276:**27981–27988.

Harris MJ, Kagawa T, Dawson PA, and Arias IM (2004) Taurocholate transport by hepatic and intestinal bile acid transporters is independent of FIC1 overexpression in Madin-Darby canine kidney cells. *J Gastroenterol Hepatol* **19:**819–825.

Huber-Ruano I and Pastor-Anglada M (2009) Transport of nucleoside analogs across the plasma membrane: a clue to understanding drug-induced cytotoxicity. *Curr Drug Metab* **10:**347–358.

Karim-Jimenez Z, Hernando N, Biber J, and Murer H (2000) Requirement of a leucine residue for (apical) membrane expression of type IIb NaPi cotransporters. *Proc Natl Acad Sci USA* **97:**2916–2921.

Kwon SH and Guggino WB (2004) Multiple sequences in the C terminus of MaxiK channels are involved in expression, movement to the cell surface, and apical localization. *Proc Natl Acad Sci USA* **101:**15237–15242.

Loewen SK, Ng AM, Yao SY, Cass CE, Baldwin SA, and Young JD (1999) Identification of amino acid residues responsible for the pyrimidine and purine nucleoside specificities of human concentrative Na(+) nucleoside cotransporters hCNT1 and hCNT2. *J Biol Chem* **274:**24475–24484.

Mackey JR, Galmarini CM, Graham KA, Joy AA, Delmer A, Dabbagh L, Glubrecht D, Jewell LD, Lai R, Lang T, et al. (2005) Quantitative analysis of nucleoside transporter and metabolism gene expression in chronic lymphocytic leukemia (CLL): identification of fludarabine-sensitive and -insensitive populations. *Blood* **105:**767–774.

Mancias JD and Goldberg J (2007) The transport signal on Sec22 for packaging into COPII-coated vesicles is a conformational epitope. *Mol Cell* **26:**403–414.

Mangravite LM, Badagnani I, and Giacomini KM (2003) Nucleoside transporters in the disposition and targeting of nucleoside analogs in the kidney. *Eur J Pharmacol* **479:**269–281.

Molina-Arcas M, Casado FJ, and Pastor-Anglada M (2009) Nucleoside transporter proteins. *Curr Vasc Pharmacol* **7:**426–434.

Moyer BD, Denton J, Karlson KH, Reynolds D, Wang S, Mickle JE, Milewski M, Cutting GR, Guggino WB, Li M, et al. (1999) A PDZ-interacting domain in CFTR is an apical membrane polarization signal. *J Clin Invest* **104:**1353–1361.

Ngo LY, Patil SD, and Unadkat JD (2001) Ontogenic and longitudinal activity of Na(+)-nucleoside transporters in the human intestine. *Am J Physiol Gastrointest Liver Physiol* **280:**G475–G481.

Nishimura N and Balch WE (1997) A di-acidic signal required for selective export from the endoplasmic reticulum. *Science* **277:**556–558.

Nishimura N, Bannykh S, Slabough S, Matteson J, Altschuler Y, Hahn K, and Balch WE (1999) A di-acidic (DXE) code directs concentration of cargo during export from the endoplasmic reticulum. *J Biol Chem* **274:**15937–15946.

Nourry C, Grant SG and Borg JP (2003) PDZ domain proteins: plug and play! *Sci STKE* **2003:**RE7.

Otte S and Barlowe C (2002) The Erv41p-Erv46p complex: multiple export signals are required in trans for COPII-dependent transport from the ER. *EMBO J* **21:**6095–6104.

Pastor-Anglada M, Cano-Soldado P, Errasti-Murugarren E, and Casado FJ (2008) SLC28 genes and concentrative nucleoside transporter (CNT) proteins. *Xenobiotica* **38:**972–994.

Pei D, Kang T, and Qi H (2000) Cysteine array matrix metalloproteinase (CA-MMP)/MMP-23 is a type II transmembrane matrix metalloproteinase regulated by a single cleavage for both secretion and activation. *J Biol Chem* **275:**33988–33997.

Ridley AJ (2001) Rho proteins: linking signaling with membrane trafficking. *Traffic* **2:**303–310.

Ritzel MW, Ng AM, Yao SY, Graham K, Loewen SK, Smith KM, Ritzel RG, Mowles DA, Carpenter P, Chen XZ, et al. (2001) Molecular identification and characterization of novel human and mouse concentrative Na^+-nucleoside cotransporter proteins (hCNT3 and mCNT3) broadly selective for purine and pyrimidine nucleosides (system cib). *J Biol Chem* **276:**2914–2927.

Saunders C and Limbird LE (1997) Disruption of microtubules reveals two independent apical targeting mechanisms for G-protein-coupled receptors in polarized renal epithelial cells. *J Biol Chem* **272:**19035–19045.

Subramanian VS, Marchant JS, Boulware MJ, and Said HM (2004) A C-terminal region dictates the apical plasma membrane targeting of the human sodium-dependent vitamin C transporter-1 in polarized epithelia. *J Biol Chem* **279:**27719–27728.

Sun AQ, Balasubramaniyan N, Liu CJ, Shahid M, and Suchy FJ (2004) Association of the 16-kDa subunit c of vacuolar proton pump with the ileal Na+-dependent bile acid transporter: protein-protein interaction and intracellular trafficking. *J Biol Chem* **279:**16295–16300.

Sun AQ, Salkar R, Sachchidanand, Xu S, Zeng L, Zhou MM, and Suchy FJ (2003) A 14-amino acid sequence with a beta-turn structure is required for apical membrane sorting of the rat ileal bile acid transporter. *J Biol Chem* **278:**4000–4009.

Symons M and Rusk N (2003) Control of vesicular trafficking by Rho GTPases. *Curr Biol* **13:**R409–R418.

Tsang RY, Santos C, Ghosh S, Dabbagh L, King K, Young J, Cass CE, Mackey JR, and Lai R (2008) Immunohistochemistry for human concentrative nucleoside transporter 3 protein predicts fludarabine sensitivity in chronic lymphocytic leukemia. *Mod Pathol* **21:**1387–1393.

Votsmeier C and Gallwitz D (2001) An acidic sequence of a putative yeast Golgi membrane protein binds COPII and facilitates ER export. *EMBO J* **20:**6742–6750.

Zuzarte M, Rinné S, Schlichthörl G, Schubert A, Daut J, and Preisig-Müller R (2007) A di-acidic sequence motif enhances the surface expression of the potassium channel TASK-3. *Traffic* **8:**1093–1100.

Address correspondence to: Dr. Marçal Pastor-Anglada, Departament de Bioquímica i Biologia Molecular, Facultat de Biologia, Universitat de Barcelona and CIBER EHD, Avda Diagonal 645, Edifici annex, Planta-1, 08028 Barcelona, Spain. E-mail: mpastor@ub.edu